

TransCAM: Transformer Attention-based CAM Refinement for Weakly Supervised Semantic Segmentation

Ruiwen Li¹, Zheda Mai², Chiheb Trabelsi¹, Zhibo Zhang¹, Jongseong Jang³, Scott Sanner¹

¹University of Toronto, ²Optimy AI, ³LG AI Research

{ruiwen.li, zheda.mai}@mail.utoronto.ca, chiheb.trabelsi@utoronto.ca,
zhibozhang@cs.toronto.edu, j.jang@lgresearch.ai, ssanner@mie.utoronto.ca

Abstract

Weakly supervised semantic segmentation (WSSS) with only image-level supervision is a challenging task. Most existing methods exploit Class Activation Maps (CAM) to generate pixel-level pseudo labels for supervised training. However, due to the local receptive field of Convolution Neural Networks (CNN), CAM applied to CNNs often suffers from partial activation — highlighting the most discriminative part instead of the entire object area. In order to capture both local features and global representations, the Conformer has been proposed to combine a visual transformer branch with a CNN branch. In this paper, we propose TransCAM, a Conformer-based solution to WSSS that explicitly leverages the attention weights from the transformer branch of the Conformer to refine the CAM generated from the CNN branch. TransCAM is motivated by our observation that attention weights from shallow transformer blocks are able to capture low-level spatial feature similarities while attention weights from deep transformer blocks capture high-level semantic context. Despite its simplicity, TransCAM achieves a new state-of-the-art performance of 69.3% and 69.6% on the respective PASCAL VOC 2012 validation and test sets, showing the effectiveness of transformer attention-based refinement of CAM for WSSS. Code is available at <https://github.com/liruiwen/TransCAM>.

1. Introduction

Semantic segmentation is a fundamental computer vision task that assigns semantic labels to every pixel in an image. Recent years have seen significant progress in deep-learning-based semantic segmentation methods [9, 31, 3]. However, these methods require an enormous amount of training data with pixel-level class labels. Such data needs massive fine-grained annotations and is expensive to obtain; hence much effort has been devoted to weakly supervised

semantic segmentation (WSSS) that intends to train a segmentation model with weak supervision such as bounding boxes [12, 24], scribbles [30], points [4], or image-level class labels [41, 6, 50, 1]. The image-level class label is the most accessible form of annotation since it already exists in large-scale datasets like ImageNet [34]. Therefore, we focus on WSSS using only image-level class labels in this work.

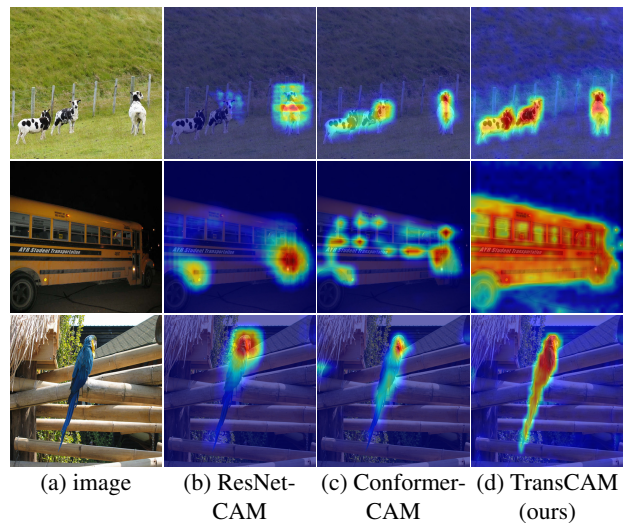


Figure 1: Comparisons of CAMs generated by different networks or methods: (a) the input images, (b) conventional CAMs generated from a ResNet-38 network (c) conventional CAMs generated from the CNN branch of a Conformer-S network (d) CAMs generated by our method.

To tackle WSSS with only image-level labels, most existing approaches rely on Class Activation Maps [51] (CAM) to generate the initial seeds for localization. Specifically, these methods often train a CNN classification network with image-level labels, from which CAM are generated and refined as pixel-level pseudo labels. Then a fully-supervised semantic segmentation network is trained using

the pseudo labels as ground-truth annotations. Clearly, the success of WSSS is critically dependent on the accuracy of the pseudo labels. However, a major obstacle of CAM-derived pseudo labels for WSSS is the partial activation issue — CAM generated by the classification model tend to highlight the most discriminative part of an object instead of the entire object area [2, 41, 6, 28] as demonstrated in Figure 1 (b). Recent work has pointed out the root cause of this issue is an intrinsic characteristic of CNNs: the local receptive field only captures small-range feature dependencies [18, 11]. Although various methods have been proposed to encourage a larger activation area aligned with the entire object region [29, 41, 42, 2, 28, 27], little work has directly addressed the local receptive field deficiencies of the CNN when applied to WSSS.

Recently, transformers [39] have demonstrated tremendous success in many computer vision tasks [14, 38], but they are much less explored for WSSS. The Vision Transformer (ViT) [14] leverages multi-head self-attention and multi-layer perceptrons to capture long-range semantic correlations, which are crucial for localizing the entire object; however, in contrast to the CNN, the ViT often ignores local feature details of objects that are also important for WSSS applications. In order to leverage advantages of both the CNN and ViT architectures, hybrid combinations of the two have been developed [43, 33, 13, 10, 47]. In particular, the Conformer [33] utilizes a CNN branch and a transformer branch to fuse local features and global representations interdependently at multiple scales.

As a first contribution of our work, we show the Conformer is more effective as a backbone for WSSS when compared to commonly used ResNets [20, 45]. As shown in Figure 1 (b) & (c), the Conformer generates CAM with more extensive coverage on the target object and more accurate pseudo labels from CAM. This leads to better WSSS performance as shown in Table 1. We believe this improvement derives from the Conformer’s ability to couple local features with global representations, which is important to alleviate the partial activation issue of CAM. Nonetheless, CAM generated from Conformer’s CNN branch are only influenced by the self-attention weights from the transformer branch in an *implicit* manner (through the Feature Coupling Units (FCU)), as shown in Figure 2, leading to poor performance on the WSSS task (Section 4.3).

To address this issue in a second contribution of our work, we propose a simple, efficient, and effective method called **TransCAM** that explicitly leverages the attention weights from the transformer branch of the Conformer to refine the CAM generated from the CNN branch. TransCAM is motivated by our observation that attention weights from the shallow transformer blocks are able to capture low-level spatial feature similarities while attention weights from deep transformer blocks capture high-level semantic con-

text (Section 4.3.3). Based on this observation, we construct an attention map that embeds both low-level and high-level spatial feature affinities by averaging the multi-head self-attention weights from all transformer blocks. The CAM generated from the CNN branch is refined by this attention map with a simple dot product. As illustrated in Figure 2, TransCAM does not rely on any additional components nor complex calculations. It simply leverages the feature affinities embedded in the Conformer backbone and enhances the CAM with a single-step dot product refinement. Thorough experiments demonstrate the effectiveness of TransCAM — despite its relative simplicity, TransCAM achieves a new state-of-the-art performance of 69.3% and 69.6% on the respective PASCAL VOC 2012 [15] validation and test sets.

We summarize our main contributions:

- We propose the first transformer-based solution (TransCAM) for WSSS to address the partial activation limitations of CAM due to the inherent deficiencies of the CNN’s local receptive field.
- TransCAM explicitly utilizes the inherent attention weights from the transformer branch of the Conformer to improve the CAM generated from the CNN branch. It is based on our observation that the attention weights capture both low-level and high-level spatial feature affinities. TransCAM does not rely on any additional components nor complex calculations, thus also making it a simple high-performance baseline for further research.
- TransCAM achieves state-of-the-art performance for WSSS on the PASCAL VOC 2012 dataset with image-level annotations.

2. Related Work

2.1. Weakly Supervised Semantic Segmentation (WSSS)

Most recent solutions to WSSS with image-level annotations use Class Activation Maps (CAM) [51] to generate the pixel-level pseudo labels and then train the segmentation model with the pseudo labels in a fully supervised manner. CAM combines the feature map before the global average pooling layer with the weights of the last fully connected layer to score and visualize the contribution of each pixel to the classification result. However, it tends to focus on the most discriminative part of the target object.

Existing works that deal with this issue are mainly divided into two categories. The first category makes the network focus on more complete object regions. Adversarial erasing [42, 21] removes the most discriminative part of an object to encourage larger activation on non-discriminative object regions; Sun *et al.* [37] explores cross-image se-

mantic relations, while Chang *et al.* leverages a sub-category objective for object pattern mining; SEAM [41] exploits consistency regularization for CAM equivalence under affine transformations; AdvCAM [28] generates an attribution map from an image that is manipulated against adversarial attack. The second category refines the initial pseudo labels for segmentation via post-processing. SEC [25] refines CAM following three principles: seed, expand, and constrain; AffinityNet [2] uses a network to predict the semantic affinity between neighboring pixels and then uses the prediction result for semantic propagation via random walk; IRNet [1] further explores the boundary activation map for determining pixel affinity; AuxSegNet [46] adopts auxiliary tasks and learns cross-task affinity to propagate the CAM. Despite the collective progress made by these works, little research has directly addressed the local receptive field deficiencies of the CNN when applied to WSSS, which is the key problem that we tackle in this work.

2.2. Self-attention for WSSS

The self-attention mechanism [39] has substantially improved various computer vision tasks including semantic segmentation. Non-local neural networks [40] apply it to convolutional neural networks to capture long-range feature dependencies. Some recent WSSS works also adopt self-attention modules to capture semantic affinities. CIAN [17] leverages self-attention to obtain more extensive and consistent activation regions from the activation maps of two images with the same class objects. SEAM [41] adopts self-attention to capture pixel affinity that can be used to refine CAM. EDAM [44] applies self-attention to model the intra-image and inter-image homogeneity. However, these methods require attaching extra components to the end of the backbone output, which increases the model complexity and ignores low-level semantic correlations. Our proposed method leverages the inherent multi-head attention weights in the transformer blocks to capture low- and high-level feature affinities.

2.3. Transformer-based Weakly Supervised Object Localization

The transformer [39] architecture is initially proposed to handle sequential data for natural language processing tasks. The Vision Transformer (ViT) [14] splits an input image into sequential patches and feeds them into the original transformer encoder to obtain the visual representation for the image classification task. TS-CAM [18] applies the visual transformer to the weakly supervised object localization task by coupling the patch token with the semantic-agnostic attention map. Although the visual transformer captures global representations, it ignores local feature details. To this end, LCTR [11] utilizes cross-patch information to enhance the local perception capability while retain-

ing global information. To date, none of these methods have been extended to WSSS.

3. Methodology

3.1. Preliminaries

3.1.1 The Conformer network

The Conformer [33] is a dual network structure aiming to couple CNN-based local features with transformer-based global representations for enhanced representation learning, as shown in Figure 2 (yellow part). Specifically, the Conformer consists of a stem module to extract initial local features, a CNN branch, a transformer branch, and Feature Coupling Units (FCUs) to progressively fuse local features in the CNN branch with global representations in the transformer branch. Note that the CNN and transformer branches have the same number of (L) repeated convolution and transformer blocks, respectively.

The first transformer block projects the output from the stem module using a convolution to generate the patch embeddings. Then, the patch embeddings are prepended with a class token, used as the input for the multi-head self-attention (MHSA) module. As for later transformer blocks, it takes the output of the FCU and adds to the token embeddings from the previous transformer block; the result concatenated with the class token is used as the input for the MHSA module. We denote the input and the output for the MHSA module in the l -th block by $X^l \in \mathbb{R}^{(1+N) \times D}$ and $\tilde{X}^l \in \mathbb{R}^{(1+N) \times D}$, where 1, N , D represents the class token, the spatial dimension of token embeddings, and transformer embedding dimensions, respectively.

The CNN branch adopts a feature pyramid structure, where the resolution of feature maps decreases with network depth while the channel number increases. Each convolution block in the CNN branch contains multiple bottlenecks, which comprises a down-projection convolution, a spatial convolution, and an up-projection convolution, following the definitions in ResNet [20].

3.1.2 Class Activation Map

A Class Activation Map (CAM) [51] for a particular class indicates the discriminative image regions used by the CNN to identify that class, which is often used to generate pseudo labels in WSSS. It can be applied to a trained classification network that contains a feature extracting network, a Global Average Pooling (GAP) layer, and a linear classification layer. The activation map is generated by multiplying the feature maps from the last convolution layer with the target-specific weights of the classification layer. The generation of the activation map that is related to the c -th class can be formulated as:

$$M_c = \theta_c^T f \quad (1)$$

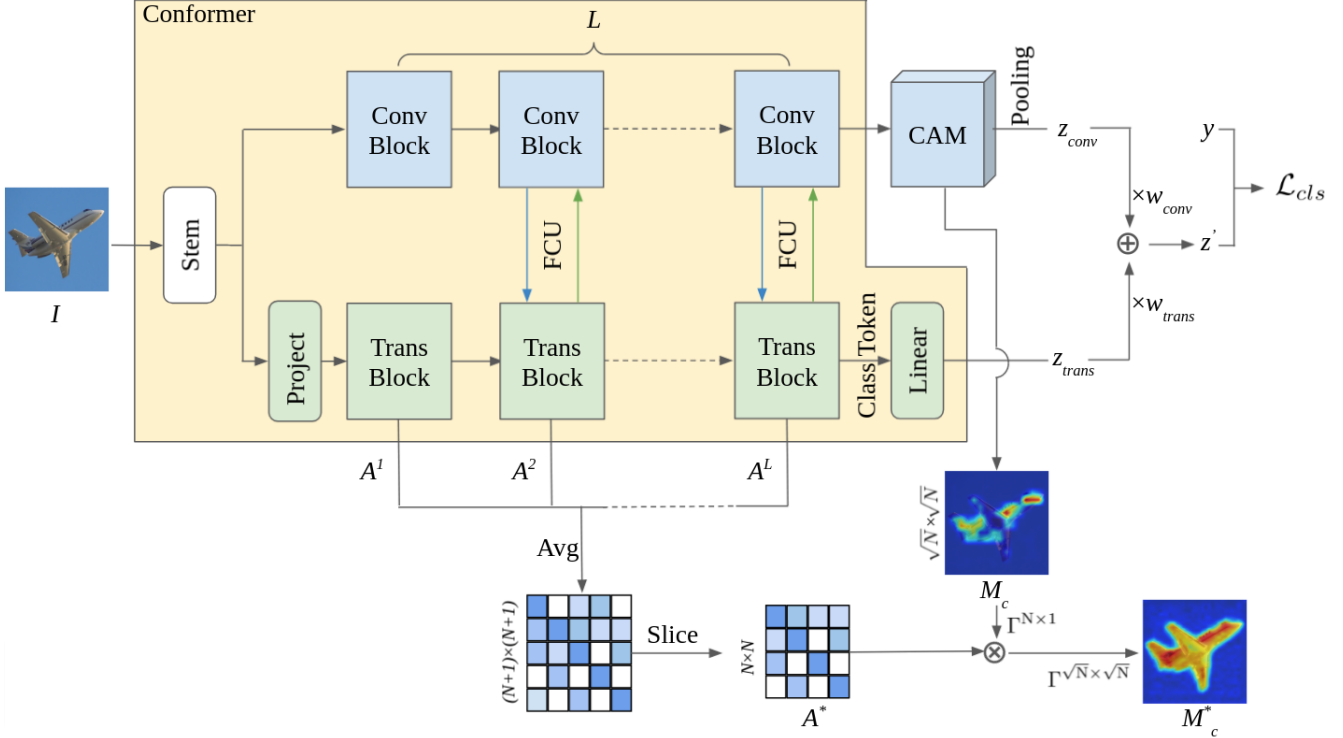


Figure 2: TransCAM leverages the dual-branch Conformer network (yellow part) with L convolution and transformer blocks. It refines the CAM M_c generated from the CNN branch with the Attention Map A^* , and the resulting CAM M_c^* has significantly improved object coverage. The Attention Map A^* is constructed by averaging the multi-head self-attention weights from all transformer blocks and excluding all the class token weights (slice). TransCAM does not rely on any additional components nor complex calculations. It simply leverages the low-level and high-level spatial feature affinities embedded in the Conformer backbone to enhance the CAM with a single-step dot product refinement.

where $M_c \in \mathbb{R}^{f_h \times f_w}$ is the class-specific activation map, $\theta_c \in \mathbb{R}^{f_c \times 1}$ are the weights of the classification layer that correspond to the c -th object, and $f \in \mathbb{R}^{f_c \times f_h \times f_w}$ is the feature map from the last convolution layer (f_c, f_h, f_w are the number of channels, the height, and the width of the feature map respectively). For WSSS, one can also implement CAM using fully convolutional networks without the linear classification layer [22].

3.2. CAM Generation from Conformer

We adopt the Conformer as the backbone network for the initial pseudo label generation. For the original Conformer network, the last bottleneck of the final convolution has a spatial convolution with stride 2 for down-scaling. We modify it with stride 1 to get higher resolution feature maps for better segmentation performance and match the size of the Attention Map described in Section 3.4. After the modification, the feature maps f from the CNN branch are of the size $f_c \times \sqrt{N} \times \sqrt{N}$ where f_c is the number of channels, and N denotes the spatial dimension of token embeddings.

CAM is an efficient method to localize objects given image class labels. We use CAM to generate the activation

map $M \in \mathbb{R}^{C \times \sqrt{N} \times \sqrt{N}}$ from the CNN branch of the Conformer where C and N are the respective number of classes (including the background class) and spatial dimension of token embeddings. As shown in Figure 1 (b) & (c), the CAM from the Conformer highlights more extensive object regions compared to the CAM from conventional CNNs [36, 20] since the Conformer employs the MHSA mechanism with the global receptive field to capture long-range feature dependencies. However, it is still hard to achieve ideal performance for the WSSS task if we directly use CAM from the Conformer for pseudo label generation since the CAM is only influenced by the self-attention weights from the transformer branch in an *implicit* manner (through FCU) and does not fully exploit the feature affinity information from the attention weights for localization.

3.3. Attention Map Generation

We assume that the weights of the multi-head self-attention module in the l -th transformer block are $A^l \in \mathbb{R}^{S \times (1+N) \times (1+N)}$, where S is the number of heads. The

attention weights A^l are computed as:

$$A^l = \text{softmax}\left(\frac{Q^l K^{l\top}}{\sqrt{D/S}}\right) \quad (2)$$

where Q^l and K^l are the key and query representations projected from X^l in the l -th transformation block. To aggregate the semantic context captured by all heads, we take the average of A^l across all heads to get $\bar{A}^l \in \mathbb{R}^{(1+N) \times (1+N)}$. $\bar{A}^l_{i,j} \in \mathbb{R}$ reveals how much the j -th input token embedding contributes to the i -th output token embedding of the MHSA module in the l -th transformer block, and \bar{A}^l (excluding the weights for the class token) captures spatial feature affinities in l -th transformation block in general.

In order to acquire a single attention map, we can compute the average attention weights $\bar{A} \in \mathbb{R}^{(1+N) \times (1+N)}$ over different transformer blocks:

$$\bar{A} = \frac{1}{L} \sum_l \bar{A}^l \quad (3)$$

To better understand what information the attention weights from different blocks capture, we compare the average attention weights in shallow blocks (first half), denoted by *AS*; deep blocks (second half), denoted by *AD* and all blocks, denoted by *AA* in Figure 3. It can be observed that *AS* tends to assign high weights to the pixels that are similar in texture to the reference point, which correlates with the fact that shallow transformer blocks leverage the local feature captured by the early convolution blocks. *AD* reveals the ability of the Attention Map to capture high-level semantics, *e.g.*, it manages to capture three persons instead of two for *AS* in the first image; it highlights the eyes and ears of the cat in the fourth image. However, it looks noisy because token embeddings in deep layers reflect complex semantic context. *AA* is able to leverage both low-level local feature similarities from shallow blocks and high-level semantic context from deep blocks. It can also smooth the noise in the attention weights from deep blocks. Based on this observation, we believe that it is crucial to combine both low-level and high-level feature affinities for CAM refinement, and therefore, we compute the average attention weights \bar{A} over all transformer blocks.

We ignore the attention weights in \bar{A} that are related to the class token since they only imply the contribution of each token embedding to the classification result but do not reflect the spatial feature affinities. The final Attention Map $A^* \in \mathbb{R}^{N \times N}$ can be computed as:

$$A^* = (\bar{A}_{i,j})_{2 \leq i \leq N+1, 2 \leq j \leq N+1} \quad (4)$$

3.4. Attention-based CAM refinement

The attention weights contain semantic information that could be leveraged to generate CAM with extensive object

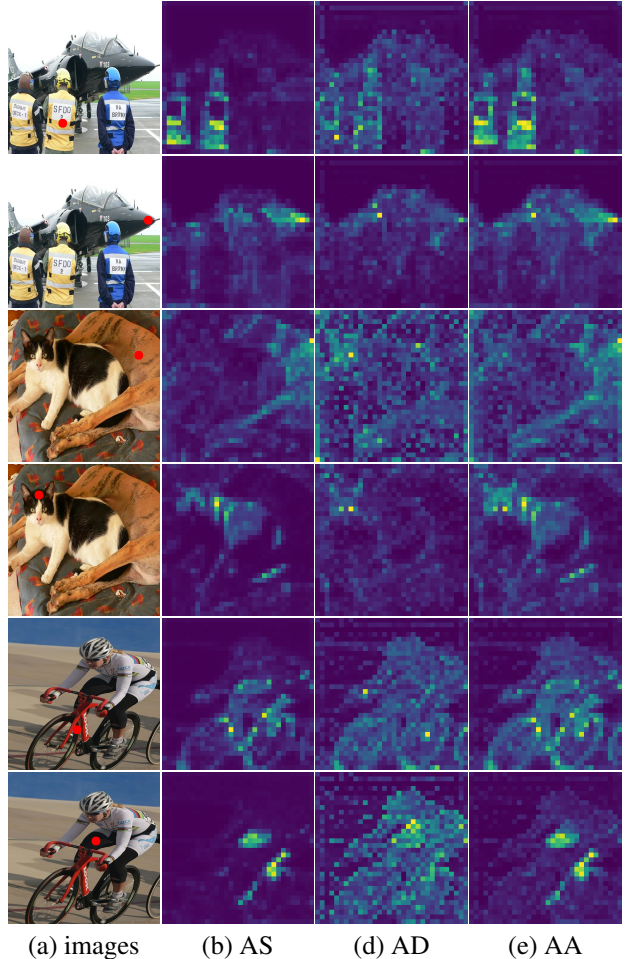


Figure 3: Visualization of input images with reference points (red dots) and the Attention Maps of the reference points. We show the Attention Maps generated by different weighting methods: averaging attention weights in shallow blocks (*AS*), deep blocks (*AD*), and all blocks (*AA*).

coverage. Multiple methods could be used to fuse the semantic information with CAM as shown in Section 4.3. We propose to leverage the spatial feature affinities captured by A^* to refine the CAM M_c via matrix multiplication:

$$M_c^* = \Gamma^{\sqrt{N} \times \sqrt{N}}(A^* \cdot \Gamma^{N \times 1}(M_c)) \quad (5)$$

where $M_c^* \in \mathbb{R}^{\sqrt{N} \times \sqrt{N}}$ is the refined CAM, $\Gamma^{N \times 1}$ is the reshape operator that flattens M_c to match the size of the patch embeddings, and $\Gamma^{\sqrt{N} \times \sqrt{N}}$ is the operator that reshapes to the dimension of M_c . M_c^* explicitly exploits the context information from the transformer attention weights and can be used to generate an initial pseudo label with extensive object coverage for the WSSS task.

3.5. Training and Pseudo Label Generation

We apply the GAP layer to the activation map M from the CNN branch to obtain the prediction vector $z_{conv} \in \mathbb{R}^C$. Following the original Conformer, we attach a linear layer to the class token at the end of the transformer branch and obtain the prediction vector $z_{trans} \in \mathbb{R}^C$. We use the weighted sum of z_{conv} and z_{trans} as the prediction logits: $z' = w_{conv}z_{conv} + w_{trans}z_{trans}$, where $z' \in \mathbb{R}^C$, $w_{conv} \in \mathbb{R}$, $w_{trans} \in \mathbb{R}$ denotes the final logits, the weight for convolution logits, the weight for transformer logits, respectively. We employ multi-label soft margin loss for network training. The classification loss defined for $C - 1$ foreground image labels is formulated as:

$$\mathcal{L}_{cls} = -\frac{1}{C-1} \sum_{c=1}^{C-1} [y_c \log\left(\frac{1}{1+e^{-z'_c}}\right) + (1-y_c) \log\left(\frac{e^{-z'_c}}{1+e^{-z'_c}}\right)] \quad (6)$$

where $z'_c \in \mathbb{R}$ is the logit of the c -th object, and $y_c \in \{0, 1\}$ is the ground truth class annotation of the c -th object. After we have the trained classification model, to generate the pseudo labels, we set the background score as:

$$M_{h,w}^{bkg} = \tau \quad (7)$$

where $\tau \in [0, 1]$ denotes the hard threshold parameter at the position (h, w) , $1 \leq h \leq H$, $1 \leq w \leq W$, H and W are the height and the width of the image. During inference, we apply elementwise min-max normalization to all refined foreground CAMs $M_{c \mid 1 \leq c \leq C-1}^*$ and concatenate them together. We up-sample the normalized result to the size of the input image, then we append M^{bkg} with the result denoted as $\hat{M}^* \in C \times H \times W$. The pixel-level pseudo label is calculated as:

$$Y_{h,w} = \operatorname{argmax}_c \hat{M}_{h,w}^* \quad (8)$$

where $Y_{h,w} \in \{1, \dots, C\}$ denotes the class label of the pixel at position h, w .

4. Experiments

4.1. Dataset and Evaluation Metric

We evaluate our method on the PASCAL VOC 2012 segmentation benchmark [15]. There are 21 object categories in the dataset, including 20 foreground objects and the background. The official dataset is split into 1464 images for training, 1449 images for validation, and 1456 images for testing. Following the conventional experimental protocol used in the previous works [41, 2, 27, 23, 50], we build an augmented train set with 10582 images by taking additional annotations from the Semantic Boundary Dataset [19]. We leverage only image-level class labels during training. To measure the performance of our method, we use the mean Intersection-over-Union (mIoU) as the evaluation metric.

4.2. Implementation Details

We adopt Conformer-S [33] with pre-trained weights on ImageNet [34] as the backbone network. The Conformer-S network has 37.7M parameters, which is less than ResNet-101 (44.5M). The dual-branch importance weights (w_{conv}, w_{trans}) are set to (0.5, 0.5), and the performance of other weights are reported in Section 4.3. Our model is trained on a single Tesla V100 GPU with 32GB RAM. We use standard data augmentations during training: random scaling, random horizontal flipping, color jittering, and random cropping. We randomly re-scale the training image in the range of [320, 640] and crop them into the size of 512×512 as the network input. We train our model for 20 epochs with the AdamW [32] optimizer and batch size 8. The learning rate is set to 0.00005, and the weight decay is set to 0.0005. During inference, aggregating prediction maps from multi-scaled input of a test image is commonly used to boost the final performance. We resize a test image into 256×256 , 512×512 , and 768×768 during inference.

4.3. Ablation Studies

We conduct ablation studies with results validated on PASCAL VOC 2012 *train* set to verify the effectiveness of our proposed approach. In all experiments, the background score τ is set to the value that gives the best mIoU for the generated pseudo labels on the *train* set in order to ensure a fair comparison.

method	mIoU (%)
ResNet-38-CAM [†]	47.16
ResNet-38-CAM [41]	47.43
ResNet-50-CAM [1]	48.30
Conformer-S-CAM	51.70

Table 1: Comparison of pseudo labels produced by CAM with different backbones. [†] denotes our implementation.

4.3.1 CAM with different backbones

In previous works, CNN models such as ResNet-38 [45] and ResNet-50 [20] are widely used to generate the initial pseudo labels. Table 1 compares the pseudo labels generated by CAM with ResNet-38, ResNet-50, and Conformer-S [33] backbone. CAM with Conformer-S outperforms CAM with ResNet-50 by 3.4%, verifying that Conformer generates CAM with more extensive object coverage. Thanks to the interactive fusion of CNN features and transformer embeddings, the Conformer captures local features and global representations; thus it serves as an effective backbone for the WSSS task.

4.3.2 Coupling CAM with attention weights

We denote our baseline: the CAM from the Conformer-S CNN branch without coupling Attention Map as *Conformer-S-CAM*. We explore different ways to leverage the context information from the attention weights for CAM refinement. One approach is to employ the attention weights A^{cls} for the class token. A^{cls} highlights the crucial pixels for image classification without focusing on local areas. Although A^{cls} is not distinguishable for object classes, we can fuse it with CAM by Hadamard product to make it aware of object categories. We denote this method as *ClsAttn*. Another approach to couple attention weights with CAM is aggregating the patch attention maps based on the patch activation values obtained from CAM, denoted by *AttnAgg*. The detailed calculations and the qualitative results of *ClsAttn* and *AttnAgg* are given in the Appendix. Table 2 shows the performance comparison of our proposed method with *Conformer-S-CAM*, *ClsAttn*, and *AttnAgg*. Both *ClsAttn* and *AttnAgg* do not have noticeable improvement from the baseline, while our proposed approach increases the mIoU by 13.15%. It verifies the effectiveness of our method that leverages spatial feature affinities for CAM refinement.

method	mIoU (%)
Conformer-S-CAM (baseline)	51.70
ClsAttn	51.15
AttnAgg	51.87
TransCAM (ours)	64.85

Table 2: Comparison with our baseline and different attention-based refinement approaches.

4.3.3 Leveraging attention weights in all blocks

There are 12 transformer blocks in the Conformer-S network. We compare different methods for generating the final Attention Map A^* : averaging attention weights in shallow blocks (Block 1-6), denoted by *AS*; deep blocks (Block 6-12), denoted by *AD*; all blocks (Block 1-12), denoted by *AA*. Table 3 shows the difference in mIoU of applying these attention weighting methods. *AA* achieves better performance than *AS* and *AD* in terms of mIoU, verifying the importance of combining low-level feature affinities and high-level semantic correlations for CAM refinement.

4.3.4 Importance weights for dual branches

We experiment with different combinations of importance weights for logits (w_{conv}, w_{trans}), which control the relative importance of the CNN branch and the transformer branch for image classification. As shown in Figure 4,

method	mIoU (%)
AS	60.39
AD	63.89
AA	64.85

Table 3: Comparison of various attention weighting methods that average attention weights from different transformer blocks.

logit weights have little impact on the pseudo label quality when $w_{conv} > 0.1$ for both our method and our baseline (*Conformer-S-CAM*). The performance is expected to be low when w_{conv} is 0 since the essential weights for CAM generation are not trained. In other experiments, we report the performance with (w_{conv}, w_{trans}) assigned to $(0.5, 0.5)$.

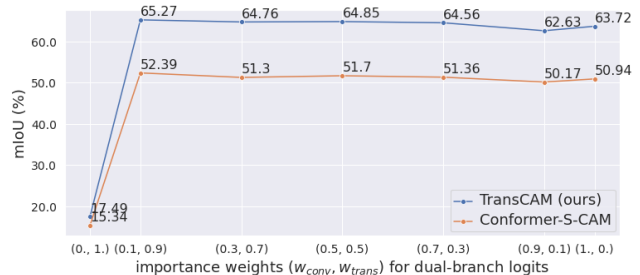


Figure 4: Impact of importance weights for dual-branch logits on the pseudo label in terms of mIoU. When $w_{conv} > 0.1$, the importance weights have little influence on the pseudo label performance.

4.4. Comparison with State-of-the-art

We adopt PSA [2] for post-processing following previous work [41, 50] to improve the mIoU of our pixel-level pseudo labels. The PSA-refined pseudo labels achieve 69.14% mIoU on the PASCAL VOC 2012 *train* set. Then, the dense CRF [26] is employed to improve the pseudo labels obtained in the previous step. The final pseudo labels achieve 70.23% mIoU on the PASCAL VOC 2012 *train* set. Table 5 compares the pseudo labels obtained by TransCAM (with and without post-processing) with other recent methods. For pseudo labels without post-processing, TransCAM outperforms others by a large margin; it has a smaller performance improvement after applying post-processing, possibly since it has already leveraged semantic affinities that PSA relies on for refinement.

We train the classical segmentation model DeepLab [8] with ResNet38 [45] backbone (pre-trained on ImageNet) on the post-processed pseudo labels in a fully-supervised manner. Table 4 shows our categorical mIoU performance on the PASCAL VOC 2012 *val* set. Figure 5 gives some qualitative semantic segmentation results on the PASCAL VOC

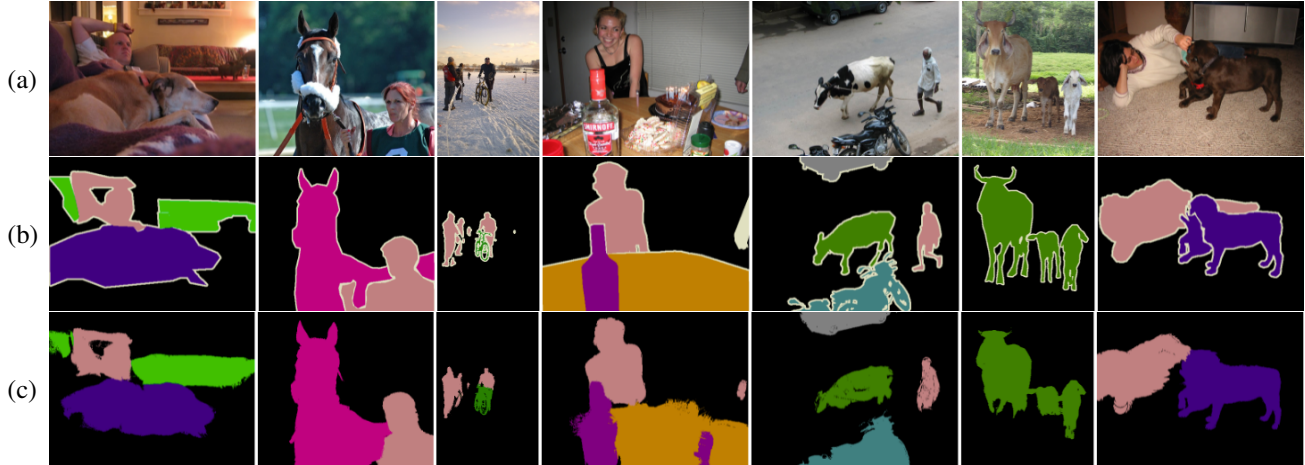


Figure 5: Qualitative semantic segmentation results on PASCAL VOC 2012 *val* set. (a) Original images; (b) Ground truth labels; (c) Prediction of the segmentation model trained on TransCAM generated pseudo labels.

method	bkg	aero	bike	bird	boat	bottle	bus	car	cat	chair	cow	table	dog	horse	mbk	person	plant	sheep	sofa	train	tv	mIoU
SEC [25]	82.4	62.9	26.4	61.6	27.6	38.1	66.6	62.7	75.2	22.1	53.5	28.3	65.8	57.8	62.3	52.5	32.5	62.6	32.1	45.4	45.3	50.7
AdvErasing [42]	83.4	71.1	30.5	72.9	41.6	55.9	63.1	60.2	74.0	18.0	66.5	32.4	71.7	56.3	64.8	52.4	37.4	69.1	31.4	58.9	43.9	55.0
PSA [2]	88.2	68.2	30.6	81.1	49.6	61.0	77.8	66.1	75.1	29.0	66.0	40.2	80.4	62.0	70.4	73.7	42.5	70.7	42.6	68.1	51.6	61.7
SEAM [41]	88.8	68.5	33.3	85.7	40.4	67.3	78.9	76.3	81.9	29.1	75.5	48.1	79.9	73.8	71.4	75.2	48.9	79.8	40.9	58.2	53.0	64.5
FickleNet [27]	89.5	76.6	32.6	74.6	51.5	71.1	83.4	74.4	83.6	24.1	73.4	47.4	78.2	74.0	68.8	73.2	47.8	79.9	37.0	57.3	64.6	64.9
Chang <i>et al.</i> [6]	88.8	51.6	30.3	82.9	53.0	75.8	88.6	74.8	86.6	32.4	79.9	53.8	82.3	78.5	70.4	71.2	40.2	78.3	42.9	66.8	58.8	66.1
Ours	91.3	81.9	35.4	84.7	67.6	67.9	87.5	80.5	86.5	31.4	73.9	52.5	84.0	74.9	74.6	79.0	44.7	84.1	47.0	78.4	46.6	69.3

Table 4: Categorical semantic segmentation performance on PASCAL VOC 2012 *val*.

Method	w/o p.p.	w/ p.p.
Mixup-CAM _{BMVC20} [5]	50.1	61.9
Chang <i>et al.</i> CVPR20 [6]	50.9	63.4
SEAM _{CVPR20} [41]	55.4	63.6
AdvCAM _{CVPR21} [28]	55.6	67.8
CPN _{ICCV21} [50]	57.4	68.0
TransCAM	64.9	70.2

Table 5: Comparison of pseudo labels with and without post-processing (p.p.) in terms of mIoU on PASCAL VOC 2012 *train* set

2012 *val* set, which shows that TransCAM performs well on some relatively hard examples where multiple objects are presented in an image. Table 6 compares the performance of TransCAM with previous methods. TransCAM achieves 69.3% and 69.6% mIoU on the PASCAL VOC 2012 *val* and *test* sets, respectively, which represents the state-of-the-art performance for approaches that adopt the ResNet38 segmentation backbone. Moreover, TransCAM performs 1% better on the *test* set than the previous state-of-the-art AugSegNet [46] method that uses additional saliency supervision.

Method	Backbone	Sup.	<i>val</i>	<i>test</i>
PSA _{CVPR18} [2]	ResNet38	\mathcal{I}	61.7	63.7
IRN _{CVPR19} [1]	ResNet50	\mathcal{I}	63.5	64.8
FickleNet _{CVPR19} [27]	ResNet101	$\mathcal{I} + \mathcal{S}$	64.9	65.3
CIAN _{AAAI20} [17]	ResNet101	\mathcal{I}	64.3	65.3
SSDD _{ICCV19} [35]	ResNet38	\mathcal{I}	64.9	65.5
SEAM _{CVPR20} [41]	ResNet38	\mathcal{I}	64.5	65.7
Chang <i>et al.</i> CVPR20 [6]	ResNet101	\mathcal{I}	66.1	65.9
BES _{ECCV20} [7]	ResNet101	\mathcal{I}	65.7	66.6
CONTA _{NIPS20} [49]	ResNet38	\mathcal{I}	66.1	66.7
MCIS _{ECCV20} [37]	ResNet101	$\mathcal{I} + \mathcal{S}$	66.2	66.9
ICD _{CVPR20} [16]	ResNet101	$\mathcal{I} + \mathcal{S}$	67.8	68.0
AdvCAM _{CVPR21} [28]	ResNet101	\mathcal{I}	68.1	68.0
Yao <i>et al.</i> CVPR21 [48]	ResNet101	$\mathcal{I} + \mathcal{S}$	68.3	68.5
CPN _{ICCV21} [50]	ResNet38	\mathcal{I}	67.8	68.5
AuxSegNet _{ICCV21} [46]	ResNet38	$\mathcal{I} + \mathcal{S}$	69.0	68.6
TransCAM (ours)	ResNet38	\mathcal{I}	69.3	69.6

Table 6: Comparison with state-of-the-art methods on PASCAL VOC *val* and *test* set in terms of mIoU (%). The Backbone refers to the segmentation network. Sup. specifies whether image-level labels (\mathcal{I}) or off-the-shelf saliency maps (\mathcal{S}) are used.

5. Conclusion

We proposed TransCAM, a transformer-CNN hybrid solution to solve limitations of class activation maps (CAM) for weakly supervised semantic segmentation (WSSS) due to partial activation that is intrinsic to the use of CNNs. Specifically, TransCAM explicitly leverages the attention weights from the transformer branch of the Conformer to refine the CAM generated from the CNN branch. TransCAM is motivated by our observation that attention weights from shallow transformer blocks are able to capture low-level spatial feature similarities while attention weights from deep transformer blocks capture high-level semantic context. Our method is simple, efficient, and effective for generating high-quality pixel-level pseudo labels as the first transformer-based approach in WSSS. Despite its simplicity, TransCAM achieves a new state-of-the-art performance on both the PASCAL VOC 2012 validation and test sets.

References

- [1] Jiwoon Ahn, Sunghyun Cho, and Suha Kwak. Weakly supervised learning of instance segmentation with inter-pixel relations. In *Proceedings of the IEEE/CVF conference on computer vision and pattern recognition*, pages 2209–2218, 2019. [1](#), [3](#), [6](#), [8](#)
- [2] Jiwoon Ahn and Suha Kwak. Learning pixel-level semantic affinity with image-level supervision for weakly supervised semantic segmentation. In *Proceedings of the IEEE conference on computer vision and pattern recognition*, pages 4981–4990, 2018. [2](#), [3](#), [6](#), [7](#), [8](#), [13](#)
- [3] Vijay Badrinarayanan, Alex Kendall, and Roberto Cipolla. Segnet: A deep convolutional encoder-decoder architecture for image segmentation. *IEEE transactions on pattern analysis and machine intelligence*, 39(12):2481–2495, 2017. [1](#)
- [4] Amy Bearman, Olga Russakovsky, Vittorio Ferrari, and Li Fei-Fei. What’s the point: Semantic segmentation with point supervision. In *European conference on computer vision*, pages 549–565. Springer, 2016. [1](#)
- [5] Yu-Ting Chang, Qiaosong Wang, Wei-Chih Hung, Robinson Piramuthu, Yi-Hsuan Tsai, and Ming-Hsuan Yang. Mixupcam: Weakly-supervised semantic segmentation via uncertainty regularization. *arXiv preprint arXiv:2008.01201*, 2020. [8](#)
- [6] Yu-Ting Chang, Qiaosong Wang, Wei-Chih Hung, Robinson Piramuthu, Yi-Hsuan Tsai, and Ming-Hsuan Yang. Weakly-supervised semantic segmentation via sub-category exploration. In *Proceedings of the IEEE/CVF Conference on Computer Vision and Pattern Recognition*, pages 8991–9000, 2020. [1](#), [2](#), [8](#)
- [7] Liyi Chen, Weiwei Wu, Chenchen Fu, Xiao Han, and Yuntao Zhang. Weakly supervised semantic segmentation with boundary exploration. In *European Conference on Computer Vision*, pages 347–362. Springer, 2020. [8](#), [13](#)
- [8] Liang-Chieh Chen, George Papandreou, Iasonas Kokkinos, Kevin Murphy, and Alan L Yuille. Semantic image segmentation with deep convolutional nets and fully connected crfs. *arXiv preprint arXiv:1412.7062*, 2014. [7](#)
- [9] Liang-Chieh Chen, George Papandreou, Iasonas Kokkinos, Kevin Murphy, and Alan L Yuille. Deeplab: Semantic image segmentation with deep convolutional nets, atrous convolution, and fully connected crfs. *IEEE transactions on pattern analysis and machine intelligence*, 40(4):834–848, 2017. [1](#)
- [10] Yinpeng Chen, Xiyang Dai, Dongdong Chen, Mengchen Liu, Xiaoyi Dong, Lu Yuan, and Zicheng Liu. Mobileformer: Bridging mobilenet and transformer. *arXiv preprint arXiv:2108.05895*, 2021. [2](#)
- [11] Zhiwei Chen, Changan Wang, Yabiao Wang, Guannan Jiang, Yunhang Shen, Ying Tai, Chengjie Wang, Wei Zhang, and Lijuan Cao. Lctr: On awakening the local continuity of transformer for weakly supervised object localization. *arXiv preprint arXiv:2112.05291*, 2021. [2](#), [3](#)
- [12] Jifeng Dai, Kaiming He, and Jian Sun. Boxesup: Exploiting bounding boxes to supervise convolutional networks for semantic segmentation. In *Proceedings of the IEEE international conference on computer vision*, pages 1635–1643, 2015. [1](#)
- [13] Zihang Dai, Hanxiao Liu, Quoc Le, and Mingxing Tan. Coatnet: Marrying convolution and attention for all data sizes. *Advances in Neural Information Processing Systems*, 34, 2021. [2](#)
- [14] Alexey Dosovitskiy, Lucas Beyer, Alexander Kolesnikov, Dirk Weissenborn, Xiaohua Zhai, Thomas Unterthiner, Mostafa Dehghani, Matthias Minderer, Georg Heigold, Sylvain Gelly, et al. An image is worth 16x16 words: Transformers for image recognition at scale. *arXiv preprint arXiv:2010.11929*, 2020. [2](#), [3](#)
- [15] Mark Everingham, Luc Van Gool, Christopher KI Williams, John Winn, and Andrew Zisserman. The pascal visual object classes (voc) challenge. *International journal of computer vision*, 88(2):303–338, 2010. [2](#), [6](#)
- [16] Junsong Fan, Zhaoxiang Zhang, Chunfeng Song, and Tieniu Tan. Learning integral objects with intra-class discriminator for weakly-supervised semantic segmentation. In *Proceedings of the IEEE/CVF Conference on Computer Vision and Pattern Recognition*, pages 4283–4292, 2020. [8](#)
- [17] Junsong Fan, Zhaoxiang Zhang, Tieniu Tan, Chunfeng Song, and Jun Xiao. Cian: Cross-image affinity net for weakly supervised semantic segmentation. In *Proceedings of the AAAI Conference on Artificial Intelligence*, volume 34, pages 10762–10769, 2020. [3](#), [8](#)
- [18] Wei Gao, Fang Wan, Xingjia Pan, Zhiliang Peng, Qi Tian, Zhenjun Han, Bolei Zhou, and Qixiang Ye. Ts-cam: Token semantic coupled attention map for weakly supervised object localization. In *Proceedings of the IEEE/CVF International Conference on Computer Vision*, pages 2886–2895, 2021. [2](#), [3](#)
- [19] Bharath Hariharan, Pablo Arbeláez, Lubomir Bourdev, Subhransu Maji, and Jitendra Malik. Semantic contours from inverse detectors. In *2011 international conference on computer vision*, pages 991–998. IEEE, 2011. [6](#)
- [20] Kaiming He, Xiangyu Zhang, Shaoqing Ren, and Jian Sun. Deep residual learning for image recognition. In *Proceed-*

- ings of the *IEEE conference on computer vision and pattern recognition*, pages 770–778, 2016. 2, 3, 4, 6
- [21] Qibin Hou, PengTao Jiang, Yunchao Wei, and Ming-Ming Cheng. Self-erasing network for integral object attention. *Advances in Neural Information Processing Systems*, 31, 2018. 2
- [22] Sangheum Hwang and Hyo-Eun Kim. Self-transfer learning for weakly supervised lesion localization. In *International conference on medical image computing and computer-assisted intervention*, pages 239–246. Springer, 2016. 4
- [23] Sanghyun Jo and In-Jae Yu. Puzzle-cam: Improved localization via matching partial and full features. In *2021 IEEE International Conference on Image Processing (ICIP)*, pages 639–643. IEEE, 2021. 6
- [24] Anna Khoreva, Rodrigo Benenson, Jan Hosang, Matthias Hein, and Bernt Schiele. Simple does it: Weakly supervised instance and semantic segmentation. In *Proceedings of the IEEE conference on computer vision and pattern recognition*, pages 876–885, 2017. 1
- [25] Alexander Kolesnikov and Christoph H Lampert. Seed, expand and constrain: Three principles for weakly-supervised image segmentation. In *European conference on computer vision*, pages 695–711. Springer, 2016. 3, 8, 13
- [26] Philipp Krähenbühl and Vladlen Koltun. Efficient inference in fully connected crfs with gaussian edge potentials. *Advances in neural information processing systems*, 24, 2011. 7
- [27] Jungbeom Lee, Eunji Kim, Sungmin Lee, Jangho Lee, and Sungroh Yoon. Ficklenet: Weakly and semi-supervised semantic image segmentation using stochastic inference. In *Proceedings of the IEEE/CVF Conference on Computer Vision and Pattern Recognition*, pages 5267–5276, 2019. 2, 6, 8
- [28] Jungbeom Lee, Eunji Kim, and Sungroh Yoon. Anti-adversarially manipulated attributions for weakly and semi-supervised semantic segmentation. In *Proceedings of the IEEE/CVF Conference on Computer Vision and Pattern Recognition*, pages 4071–4080, 2021. 2, 3, 8
- [29] Kunpeng Li, Ziyang Wu, Kuan-Chuan Peng, Jan Ernst, and Yun Fu. Tell me where to look: Guided attention inference network. In *Proceedings of the IEEE Conference on Computer Vision and Pattern Recognition*, pages 9215–9223, 2018. 2
- [30] Di Lin, Jifeng Dai, Jiaya Jia, Kaiming He, and Jian Sun. Scribblesup: Scribble-supervised convolutional networks for semantic segmentation. In *Proceedings of the IEEE conference on computer vision and pattern recognition*, pages 3159–3167, 2016. 1
- [31] Jonathan Long, Evan Shelhamer, and Trevor Darrell. Fully convolutional networks for semantic segmentation. In *Proceedings of the IEEE conference on computer vision and pattern recognition*, pages 3431–3440, 2015. 1
- [32] Ilya Loshchilov and Frank Hutter. Decoupled weight decay regularization. *arXiv preprint arXiv:1711.05101*, 2017. 6
- [33] Zhiliang Peng, Wei Huang, Shanzhi Gu, Lingxi Xie, Yaowei Wang, Jianbin Jiao, and Qixiang Ye. Conformer: Local features coupling global representations for visual recognition. In *Proceedings of the IEEE/CVF International Conference on Computer Vision*, pages 367–376, 2021. 2, 3, 6
- [34] Olga Russakovsky, Jia Deng, Hao Su, Jonathan Krause, Sanjeev Satheesh, Sean Ma, Zhiheng Huang, Andrej Karpathy, Aditya Khosla, Michael Bernstein, et al. Imagenet large scale visual recognition challenge. *International journal of computer vision*, 115(3):211–252, 2015. 1, 6, 12
- [35] Wataru Shimoda and Keiji Yanai. Self-supervised difference detection for weakly-supervised semantic segmentation. In *Proceedings of the IEEE/CVF International Conference on Computer Vision*, pages 5208–5217, 2019. 8, 13
- [36] Karen Simonyan and Andrew Zisserman. Very deep convolutional networks for large-scale image recognition. *arXiv preprint arXiv:1409.1556*, 2014. 4
- [37] Guolei Sun, Wenguan Wang, Jifeng Dai, and Luc Van Gool. Mining cross-image semantics for weakly supervised semantic segmentation. In *European conference on computer vision*, pages 347–365. Springer, 2020. 2, 8
- [38] Hugo Touvron, Matthieu Cord, Matthijs Douze, Francisco Massa, Alexandre Sablayrolles, and Hervé Jégou. Training data-efficient image transformers & distillation through attention. In *International Conference on Machine Learning*, pages 10347–10357. PMLR, 2021. 2
- [39] Ashish Vaswani, Noam Shazeer, Niki Parmar, Jakob Uszkoreit, Llion Jones, Aidan N Gomez, Łukasz Kaiser, and Illia Polosukhin. Attention is all you need. *Advances in neural information processing systems*, 30, 2017. 2, 3
- [40] Xiaolong Wang, Ross Girshick, Abhinav Gupta, and Kaiming He. Non-local neural networks. In *Proceedings of the IEEE conference on computer vision and pattern recognition*, pages 7794–7803, 2018. 3
- [41] Yude Wang, Jie Zhang, Meina Kan, Shiguang Shan, and Xilin Chen. Self-supervised equivariant attention mechanism for weakly supervised semantic segmentation. In *Proceedings of the IEEE/CVF Conference on Computer Vision and Pattern Recognition*, pages 12275–12284, 2020. 1, 2, 3, 6, 7, 8
- [42] Yunchao Wei, Jiashi Feng, Xiaodan Liang, Ming-Ming Cheng, Yao Zhao, and Shuicheng Yan. Object region mining with adversarial erasing: A simple classification to semantic segmentation approach. In *Proceedings of the IEEE conference on computer vision and pattern recognition*, pages 1568–1576, 2017. 2, 8
- [43] Haiping Wu, Bin Xiao, Noel Codella, Mengchen Liu, Xiyang Dai, Lu Yuan, and Lei Zhang. Cvt: Introducing convolutions to vision transformers. In *Proceedings of the IEEE/CVF International Conference on Computer Vision*, pages 22–31, 2021. 2
- [44] Tong Wu, Junshi Huang, Guangyu Gao, Xiaoming Wei, Xiaolin Wei, Xuan Luo, and Chi Harold Liu. Embedded discriminative attention mechanism for weakly supervised semantic segmentation. In *Proceedings of the IEEE/CVF Conference on Computer Vision and Pattern Recognition*, pages 16765–16774, 2021. 3
- [45] Zifeng Wu, Chunhua Shen, and Anton Van Den Hengel. Wider or deeper: Revisiting the resnet model for visual recognition. *Pattern Recognition*, 90:119–133, 2019. 2, 6, 7

- [46] Lian Xu, Wanli Ouyang, Mohammed Bennamoun, Farid Boussaid, Ferdous Sohel, and Dan Xu. Leveraging auxiliary tasks with affinity learning for weakly supervised semantic segmentation. In *Proceedings of the IEEE/CVF International Conference on Computer Vision*, pages 6984–6993, 2021. [3](#), [8](#)
- [47] Yufei Xu, Qiming Zhang, Jing Zhang, and Dacheng Tao. Vi-tae: Vision transformer advanced by exploring intrinsic inductive bias. *Advances in Neural Information Processing Systems*, 34, 2021. [2](#)
- [48] Yazhou Yao, Tao Chen, Guo-Sen Xie, Chuanyi Zhang, Fumin Shen, Qi Wu, Zhenmin Tang, and Jian Zhang. Non-salient region object mining for weakly supervised semantic segmentation. In *Proceedings of the IEEE/CVF Conference on Computer Vision and Pattern Recognition*, pages 2623–2632, 2021. [8](#)
- [49] Dong Zhang, Hanwang Zhang, Jinhui Tang, Xian-Sheng Hua, and Qianru Sun. Causal intervention for weakly-supervised semantic segmentation. *Advances in Neural Information Processing Systems*, 33:655–666, 2020. [8](#)
- [50] Fei Zhang, Chaochen Gu, Chenyue Zhang, and Yuchao Dai. Complementary patch for weakly supervised semantic segmentation. In *Proceedings of the IEEE/CVF International Conference on Computer Vision*, pages 7242–7251, 2021. [1](#), [6](#), [7](#), [8](#)
- [51] Bolei Zhou, Aditya Khosla, Agata Lapedriza, Aude Oliva, and Antonio Torralba. Learning deep features for discriminative localization. In *Proceedings of the IEEE conference on computer vision and pattern recognition*, pages 2921–2929, 2016. [1](#), [2](#), [3](#)

A. Attention weights coupling approaches

This section provides additional discussion and compares TransCAM with two approaches to explicitly couple CAM with attention weights as mentioned in Section 4.3: *ClsAttn* and *AttnAgg*. *ClsAttn* employs the attention weights for the class token while *AttnAgg* aggregates the attention weights based on the activation scores from CAM. Figure 6 illustrates these two attention weight coupling approaches with the detailed calculation provided below:

A.1. ClsAttn

We employ the attention weights A^{cls} that attribute to the class token:

$$A^{cls} = (\bar{A}_{i,j})_{i=1,2 \leq j \leq N+1} \quad (9)$$

Recall that \bar{A} represents the average of the self-attention weights across all blocks and all heads, and $\bar{A}_{i,j}$ denotes on average how much the j -th input token embedding contributes to the i -th output token embedding in all layers. $A^{cls} \in \mathbb{R}^{1 \times N}$ highlights the crucial pixels for image classification (mainly highlights foreground objects), however, it is class-agnostic (indistinguishable for different target classes). We fuse it with the CAM M_c via Hadamard product to make it aware of object categories:

$$M_c^{ClsAttn} = \Gamma^{\sqrt{N} \times \sqrt{N}}(A^{cls}) \odot M_c \quad (10)$$

where $M_c^{ClsAttn}$ is the CAM coupled with attention weights by *ClsAttn*.

A.2. AttnAgg

We assume that $(A^*)^\top = [A_1^*; A_2^*; \dots; A_N^*]$, where $A_i^* \in \mathbb{R}^{N \times 1}$ denotes the attention weights (excluding class token weights) that attribute to the i -th token, highlighting the pixels correlated to the i -th patch. We aggregate A_i^* based on the activation score of the i -th patch, which is determined by the value at the i -th location of the CAM M_c :

$$M_c^{AttnAgg} = \Gamma^{\sqrt{N} \times \sqrt{N}} \left(\sum_i (\Gamma^N M_c)_i A_i^* \right) \quad (11)$$

Compared with the class-agnostic attention weights A^* , $M_c^{AttnAgg}$ is aware of object categories and facilitates better object localization ability.

Figure 7 shows the qualitative comparison of the activation maps generated by *ClsAttn*, *AttnAgg*, and TransCAM. *ClsAttn* usually leads to under-activated CAMs due to possible extreme values at local areas. *AttnAgg* leads to more extensive object coverage but at the risk of highlighting irrelevant objects since it relies on the class-agnostic attention weights for localization to a large extent. The result verifies TransCAM to be the most proper attention weights coupling approach for the WSSS task.

B. Performance with Different Conformer Architectures

In this section, we evaluate the initial pseudo label performance generated by TransCAM with different ImageNet[34] pre-trained Conformer architectures: Conformer-Ti, Conformer-S, and Conformer-B. These architectures mainly differ in terms of CNN and transformer embedding dimensions, and the number of heads for the multi-head self-attention modules. Table 7 shows these architectures, the number of parameters, the ImageNet top-1 validation accuracy, and their performance on PASCAL VOC *train* set. Conformer-S outperforms the smaller size Conformer-Ti by 6.01% mIoU. However, Conformer-B leads to a slight drop in mIoU (0.47%), although it has more parameters and higher pretraining accuracy. Our result shows that Conformer-S is the best architecture for TransCAM, considering the model size and mIoU performance.

architecture	params (M)	acc. (%)	mIoU (%)
Conformer-Ti	23.5	81.3	58.84
Conformer-S	37.7	83.4	64.85
Conformer-B	83.3	84.1	64.38

Table 7: Comparison of different ImageNet-pre-trained Conformer architectures along with their number of parameters and pretraining accuracy.

C. Additional Semantic Segmentation Results

This section includes additional semantic segmentation results that we did not have space to include in the main paper. Table 8 shows the categorical semantic segmentation performance on PASCAL VOC 2012 *test* set. In 13 out of 21 classes, TransCAM outperforms other compared methods.

method	bkg	aero	bike	bird	boat	bottle	bus	car	cat	chair	cow	table	dog	horse	mbk	person	plant	sheep	sofa	train	tv	mIoU
SEC [25]	83.5	56.4	28.5	64.1	23.6	46.5	70.6	58.5	71.3	23.2	54.0	28.0	68.1	62.1	70.0	55.0	38.4	58.0	39.9	38.4	48.3	51.7
PSA [2]	89.1	70.6	31.6	77.2	42.2	68.9	79.1	66.5	74.9	29.6	68.7	56.1	82.1	64.8	78.6	73.5	50.8	70.7	47.7	63.9	51.1	63.7
SSDD [35]	89.5	71.8	31.4	79.3	47.3	64.2	79.9	74.6	84.9	30.8	73.5	58.2	82.7	73.4	76.4	69.9	37.4	80.5	54.5	65.7	50.3	65.5
BES[7]	89.0	72.7	30.4	84.6	47.5	63.0	86.8	80.7	85.2	30.1	76.5	56.4	81.8	79.9	77.0	67.8	48.6	82.3	57.2	54.0	46.7	66.6
Ours	91.2	82.2	36.2	89.8	57.8	65.1	85.7	81.5	84.2	28.3	77.4	55.9	82.1	80.0	78.9	76.5	48.0	84.7	57.2	72.7	45.8	69.6

Table 8: Categorical semantic segmentation performance on PASCAL VOC 2012 *test* set.

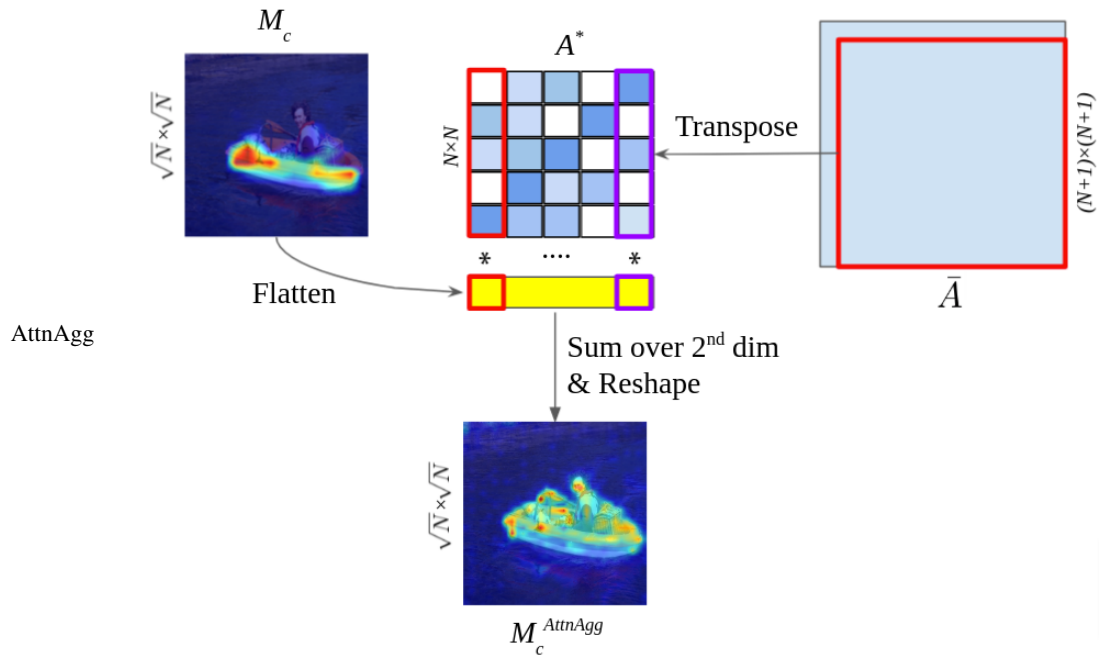
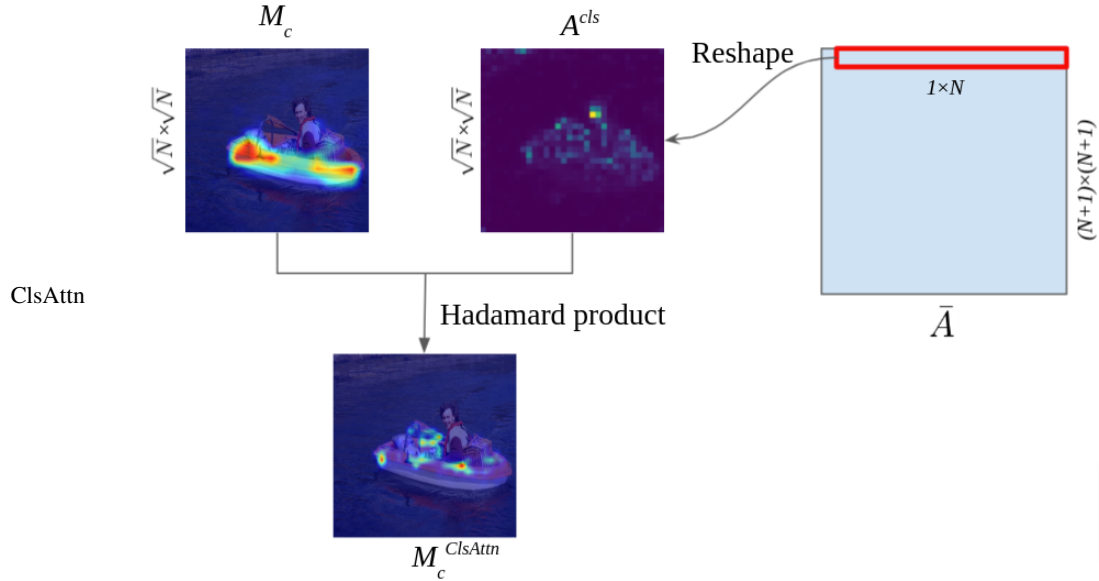


Figure 6: *ClsAttn* couples CAM with attention weights that corresponds to the class token via Hadamard product; *AttnAgg* aggregates the patch attention weights based on the corresponding activation score from CAM.

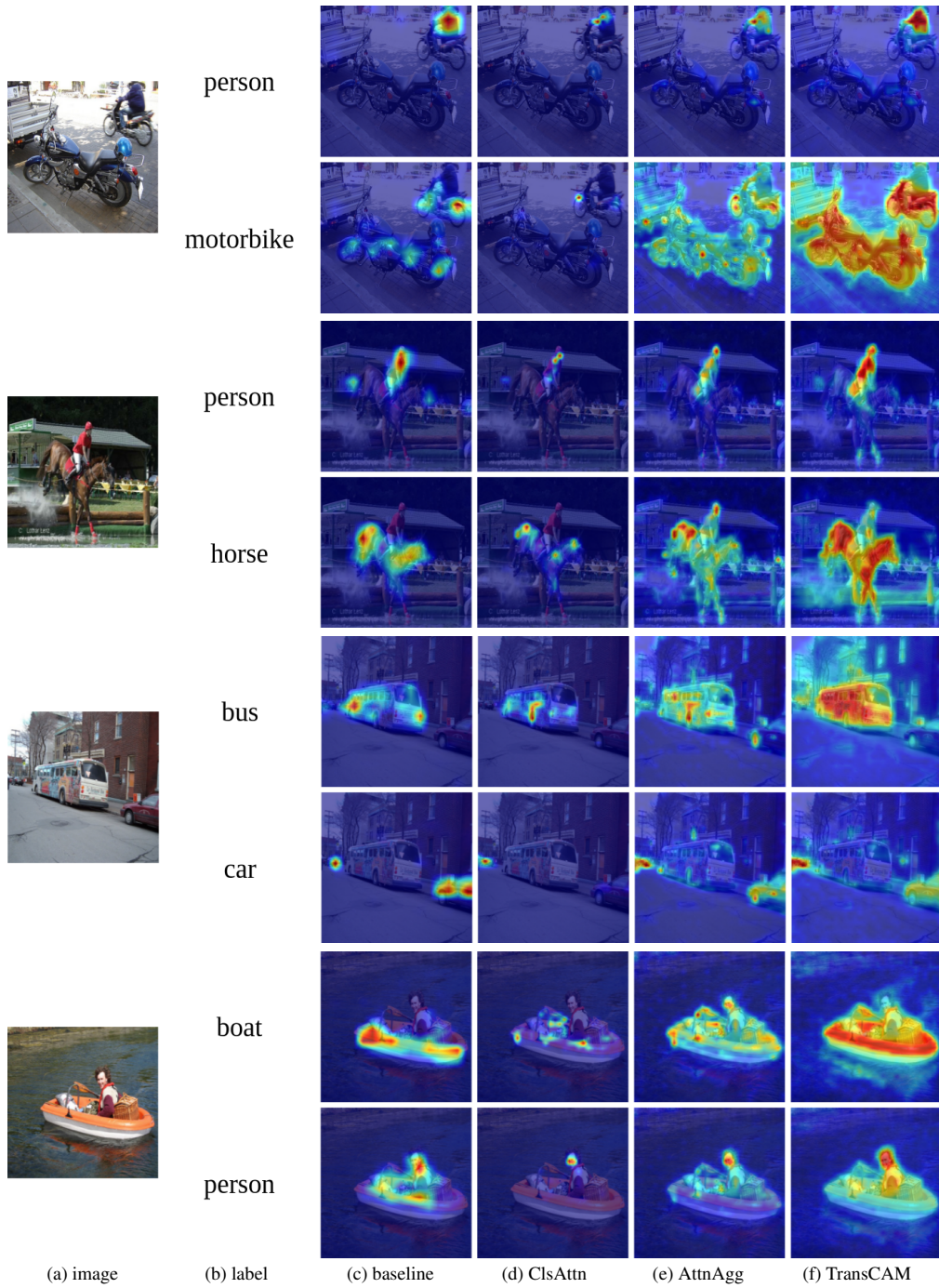


Figure 7: Qualitative comparison of different attention coupling methods. (a) input image; (b) the target class label; (c) Conformer-S-CAM (baseline); (d) ClsAttn; (e) AttnAgg; (f) TransCAM (ours)